Inflammatory Responses Induced by the Monophasic Variant of Salmonella Typhimurium in Pigs Play a Role in the High Shedder Phenotype and Fecal Microbiota Composition

Florent Kempf, Guido Cordoni, Anne-Marie Chaussé, Rosanna Drumo, Helen Brown, Daniel Horton, Frédéric Paboeuf, Martine Denis, Philippe Velge, Roberto La Ragione, et al.

AMERICAN SOCIETY FOR MICROBIOLOGY | Applied and Environmental Microbiology®

GENETICS AND MOLECULAR BIOLOGY

Improved DNA Amplification of the Hallmark IS*900* Element in *Mycobacterium avium* subsp. *paratuberculosis*: a Reexamination Based on Whole-Genome Sequence Analysis

John P. Bannantine,[a] Judith R. Stabel,[a] Darrell O. Bayles,[a] Franck Biet[b]

[a]USDA-Agricultural Research Service-National Animal Disease Center, Ames, Iowa, USA
[b]INRAE, ISP, Université de Tours, Nouzilly, France

ABSTRACT Amplification of the IS*900* multicopy element is a hallmark nucleic acid-based diagnostic test for *Mycobacterium avium* subsp. *paratuberculosis*, which causes Johne's disease in ruminants. This assay is frequently used to determine the presence of the bacterium in feces of infected cattle and sheep. Two IS*900* primer sets developed in the 1990s were widely used for decades, and their use has continued in current studies. However, these primers were developed prior to the availability of complete genome sequences. Recent sequence analysis of the binding locations for one primer pair (P90/P91) identified errors and binding inefficiencies that can be easily corrected to further increase detection sensitivity. The P90 primer is missing two nucleotides that should be present near the 3′ end, and it does not bind all copies of IS*900* due to 5′ deletions at some IS*900* loci. These IS*900* primer pairs, along with newly developed primers, were tested by real-time PCR on purified genomic DNA to determine which primer set performed the best and how primer design errors affect amplification efficiencies. The newly designed PCR primer set (JB5) showed increased sensitivity by two to three quantification cycles using purified genomic DNA and was similar in efficiency to 150C/921. These tests were extended using DNA from feces and tissues of infected cows, which showed similar results. Finally, a 167-bp partial duplication of IS*900* was found in type I strains. Although P90 and P91 primers successfully amplify *M. avium* subsp. *paratuberculosis* DNA, their use should be discontinued in favor of more efficient primer pairs in future studies.

IMPORTANCE This study is an example of how applied genomic analysis can aid diagnostic test improvements. Detection of *Mycobacterium avium* subsp. *paratuberculosis* infection of livestock prior to the appearance of clinical disease signs is very difficult but essential for identifying animals shedding the bacterium to prevent transmission of Johne's disease. Total *M. avium* subsp. *paratuberculosis* quantity in the feces as determined by real-time PCR (qPCR) using the IS*900* target indicates bacterial shedding status and potential for transmission of the pathogen. However, legacy primers designed prior to the availability of complete genome sequences that are used in these tests to detect *M. avium* subsp. *paratuberculosis* were based on data from only a single copy of IS*900* and not considering all copies collectively as a group. This approach resulted in primer design errors which can be easily corrected to improve test sensitivities. We tested original primers that contain these errors and their corrected versions by qPCR and showed improved sensitivity on purified genomic DNA as well as fecal and tissue samples. These findings may help detect the organism from environmental samples on farms where sensitivity is currently lacking.

KEYWORDS *Mycobacterium avium* subsp. *paratuberculosis*, IS*900*, fecal PCR test, genome analysis, Johne's disease, *Mycobacterium paratuberculosis*

Editor Martha Vives, Unversidad de los Andes

Address correspondence to John P. Bannantine, john.bannantine@usda.gov.

The authors declare no conflict of interest.

Received 28 September 2022
Accepted 8 January 2023
Published 31 January 2023

Mobile genetic elements are a primary driver in chromosome remodeling and no genome from extracellular bacteria is devoid of them. In the pregenomic era, the insertion sequence, termed IS*900*, was identified as a repetitive DNA element that is uniquely present in *Mycobacterium avium* subsp. *paratuberculosis*, which causes Johne's disease in cattle and other ruminants. A member of the IS*110* family of transposases (1, 2), the number of IS*900* copies in the *M. avium* subsp. *paratuberculosis* genome ranges between 16 and 22 (3, 4). Because IS*900* is *M. avium* subsp. *paratuberculosis* specific and present in multiple copies per genome, it enables high sensitivity of detection down to 1 fg of purified genomic DNA (5). This insertion sequence is 1,453 bp and contains one open reading frame, originally termed p43 (6). IS*900* is distributed randomly around the chromosome and does not have detectable regions of high insertion density. Finally, IS*900* rarely inserts within a coding sequence since it was found to disrupt only three genes among the three representative strain types (4). These strain types include type I and type III strains, typically isolated from sheep, and type II strains, typically isolated from cattle.

The IS*900* PCR test is broadly used for most Johne's disease diagnostic, genotyping and research applications. This one test has historically been used more to detect *M. avium* subsp. *paratuberculosis* infection and aid in the control of Johne's disease than any other method. This test is recommended by the World Organization for Animal Health (OIE [7]) and is more sensitive than histopathology, acid-fast staining, or culture. IS*900* was first described in *M. avium* subsp. *paratuberculosis* by two independent groups (8, 9), each of which realized early on the diagnostic implications of their discovery. *M. avium* subsp. *paratuberculosis* causes Johne's disease in cattle, sheep, and goats, and this bacterium is shed in the feces of infected animals during the advanced stages of disease. Before the discovery of this *M. avium* subsp. *paratuberculosis*-specific insertion sequence, the bacterium was only detectable by protracted culture of feces from diseased animals. Now IS*900* amplification assays are most used to detect *M. avium* subsp. *paratuberculosis* in feces of infected cattle, sheep and goats, resulting in more rapid and reliable results (10, 11). Furthermore, it is also used for organism detection in milk (12–14) and human tissues of Crohn's disease patients (15). IS*900* restriction fragment length polymorphism has emerged as a useful strain typing tool (16) that has been automated for ease of use (4).

Although IS*900* amplification is a sensitive test to determine the presence of *M. avium* subsp. *paratuberculosis* in samples, there is still a need to further optimize its sensitivity to survey *M. avium* subsp. *paratuberculosis* at the herd level on farms. Currently, environmental sampling on farms does not have sufficient sensitivity to consistently detect *M. avium* subsp. *paratuberculosis*, especially on smaller farm operations (17, 18). Efforts to improve the sensitivity of the IS*900* PCR assay include a fecal DNA extraction procedure (19, 20), *M. avium* subsp. *paratuberculosis* enrichment steps (21) and multiplex PCR approaches (22). However, no studies have examined the effect of primer binding characteristics on assay improvement. Selection of the target region and associated primer pairs should be performed with care to ensure optimal specificity and sensitivity of the assay. Using suboptimal primer pairs would theoretically lead to an under-representation of bacterial burden in feces or false-negative and false-positive reactions.

After the initial discovery of IS*900* in the late 1980s, primer sequences were soon developed to amplify this repetitive sequence (1, 23). These legacy primers were designed using sequence data from only a single copy of IS*900* rather than considering all copies collectively as a group. These early primers were then established and used in over 400 *M. avium* subsp. *paratuberculosis* studies through the decades. The diversity of IS*900* loci was recently examined by our group and demonstrated that IS*900* has several polymorphisms, especially at the 5′ end of the element (4). When comparing the IS*900* sequence among the three strain types of *M. avium* subsp. *paratuberculosis*, there are three single nucleotide polymorphisms (SNPs), as well as deletions at four total loci: two in type II, one in type III, and one in type I (4). In this study, we analyzed commonly used primer pairs to show that not every IS*900* loci contains a binding sequence for some commonly used IS*900* primers.

It is well known that high specificity in primer sequence design is critical to prevent mispriming in the target sequence. General guidelines for good primer design include a

TABLE 1 IS*900* primers and probe used in this study[a]

Primer or probe	Orientation	Sequence (5′–3′)	Δ*G*	T_m (°C)	Length	%G+C	Comment
P90	F	GAAGGGTGTTCGGGGCCGTCGCTTAGG	42.4	67.3	27	67	P90 primer reported by Millar et al. (12).
P90Corr	F	GAAGGGTGTTCGGGGCCGTCGGCCTTAGG	46.6	70.0	29	69	Corrected P90 primer for IS*900* amplification.
P91	R	GGCGTTGAGGTCGATCGCCCACGTGAC	42.9	67.3	27	67	From Millar et al. (12).
JB5F	F	GTCGTCTGCTGGGTTGATCT	26.5	53.8	20	55	Designed in this study.
JB5R	R	ATGAGCAAGGCGATCAGCAA	26.8	51.8	20	50	Designed in this study.
150C	F	CCGCTAATTGAGAGATGCGATTGG	32.2	57.4	24	50	From Vary et al. (1).
921	R	AATCAACTCCAGCAGCGCGGCCTCG	39.3	64.2	25	64	From Vary et al. (1).
Dual-labeled probe	R	FAM/TCCACGCCCGCCCAGACAGG/TAMSp	31.9	62.0	20	75	Fluorescent probe from IS*900* (1).

[a]F, forward; R, reverse. Δ*G*, free energy of the primer in 1 M NaCl at 25°C and pH 7. T_m, melting temperature under standard conditions at pH 7.

17- to 21-bp length with low secondary structure and similar melting temperatures between the primer pairs. There are several online primer design tools that account for these characteristics and more (24, 25). Primer3 software, in particular, has incorporated detailed thermodynamic algorithms and added DNA duplex stability data in the 2012 revision (26). We tested commonly used IS*900* primers and designed a new set of primers for testing the effects of primers on IS*900* amplification efficiencies.

RESULTS

Errors in IS*900* primer pairs used in Johne's disease and Crohn's disease studies. We recently analyzed the distribution and polymorphisms of every IS*900* loci in closed *M. avium* subsp. *paratuberculosis* genome sequences representing each of the three subtypes (4). Subsequently, it became of interest to apply those results to the improvement of IS*900* DNA amplification, which may lead to improved *M. avium* subsp. *paratuberculosis*. There are two primer sets that predominate in Johne's disease and Crohn's disease studies. These primer pairs were first reported by Vary et al. (1) (designated 150C and 921) and by Moss et al. (23) (designated P90 and P91). These primer pairs target a single stretch of overlapping DNA within 430 bp of the 5′ end of the element (see Fig. S1). The 5′ region of IS*900* is considered more specific to *M. avium* subsp. *paratuberculosis* (27, 28). See Table 1 for primer sequences and other characteristics. Combined, these two primer sets have been used in over 400 published *M. avium* subsp. *paratuberculosis* studies.

Analysis of 220 IS*900* loci from 14 closed *M. avium* subsp. *paratuberculosis* genomes (see Table S2) revealed that the P90 primer is missing two nucleotides, guanine and cytosine, at positions −7 and −8 from the 3′ end (Fig. 1). Furthermore, this primer error appears to have been left uncorrected in subsequent studies as suggested by at least 82 published studies that used this primer (see Table S1). Note that there are slight differences in the primer length reported in a few studies and sometimes there is a minor shifting of the binding region; however, they all overlap the originally designed P90 sequence, and none contain the GC dinucleotide (see Table S1). The IS*900* sequence originally published by Green et al. (8) also lacks the GC dinucleotide (top sequence in Fig. 1), and the P90 primer was designed based on that sequence. However, these two nucleotides are present in all other IS*900* sequences in public sequence databases. This missing dinucleotide was originally noted by Semret et al. (29) when comparing the original IS*900* sequence from Green et al. (8) with later sequence data, but they did not mention its effect on P90 primer binding. There are four other SNPs between the originally published sequence and that from the K-10 genome sequence (see Fig. S2), but these SNPs do not affect any IS*900* primer binding regions (see Fig. S1). Therefore, in this study, we designed a new primer, termed P90Corr, that includes the two nucleotides missing from the original P90 primer (Fig. 1).

Legacy IS*900* primers do not bind to every copy of IS*900*. The two commonly used IS*900* primer pairs designed in the Moss et al. (23) and Vary et al. (1) studies were analyzed at each IS*900* loci *in silico* using PrimerProspector (30). Primers designed in this study (JB5F and JB5R; see Table 2) were also included in the analysis. All primers except P90 and P90Corr yielded a theoretically optimal weighted score of 0 (Fig. 2). P90 showed the previously identified mismatches in PrimerProspector analysis, and no binding at four independent IS*900* loci, indicated by the 5+ weighted score in Fig. 2. When P90Corr is analyzed

```
                                                    -8      -1
Original IS900 seq = GAAGGGTGTTCGGGGCCGTCG--CTTAGG
    P90 primer seq = GAAGGGTGTTCGGGGCCGTCG--CTTAGG
P90Corr primer seq = GAAGGGTGTTCGGGGCCGTCGGCCTTAGG
   K-10 Genome seq = GAAGGGTGTTCGGGGCCGTCGGCCTTAGG
```

FIG 1 The P90 and P90Corr primer sequences are shown in context with the originally reported IS*900* sequence from Green et al. (8) (top sequence) and the *M. avium* subsp. *paratuberculosis* K-10 genome sequence from locus 1 (bottom sequence; genome coordinates 39820 to 39848 from GCF_000007865.1). Shown in the middle is the original P90 primer sequence, as published by Moss et al. (23) and used in many other research studies (see Table S1). Note that both the original IS*900* sequence and the P90 primer are missing the GC dinucleotide at positions −7 and −8 from the 3′ end. The P90Corr primer, which represents the corrected P90 primer, contains the GC dinucleotide (shown in red) and matches the K-10 genome sequence exactly. Selected nucleotide positions are marked along the top row with −1 defining the 3′-end nucleotide.

in PrimerProspector, mismatches are no longer present, but there is still a lack of binding at four IS*900* loci (Fig. 2). The four IS*900* variants not expected to bind the P90 or P90Corr primers are due to specific deletions in IS*900* variants distributed differentially across type I, II, and III strains.

As stated previously, a full-length copy of IS*900* is 1,453 bp. An alignment of all IS*900* loci from the representative type I, II, and III *M. avium* subsp. *paratuberculosis* strains shows deletions at 6 of the 58 total IS*900* sites (4). These include a 5-bp deletion in locus 9 of the type I strain and locus 13 of the type III strain (Fig. 3). In addition, there is a 44-bp deletion in one of the copies from each strain type, and a 70-bp deletion in locus 17 of the type II strains. All deletions occur toward the start of each locus and the 44- and 70-bp deletions prevent P90 and P90Corr primer binding at those loci (Fig. 3). There are also three SNPs at positions 169, 216, and 1405 (4, 29, 31); however, none of these SNPs affect primer binding for any of the IS*900* primers in this study. Because genomic sequence corresponding to P90 binding in the K-10 strain is absent at 2 of the 17 loci, only 15 copies would be expected to amplify.

This analysis was conducted on representative genome sequences; however, we wanted to determine whether these findings would remain true when analyzing all available closed *M. avium* subsp. *paratuberculosis* genome sequences. Therefore, our analysis was expanded to 14 complete *M. avium* subsp. *paratuberculosis* genome sequences to identify all IS*900* primer binding sites. Examination of every IS*900* loci within these *M. avium* subsp. *paratuberculosis* genomes in the context of commonly used primer binding sites revealed new findings summarized in Table S2 in the supplemental material. Notably, the 44-bp deletion was found in all 14 genomes analyzed. In addition, the final locus in all type II strains analyzed showed the same 70-bp deletion as that observed in K-10 locus 17 (Fig. 3).

Partial duplication of IS*900* in a subset of *M. avium* subsp. *paratuberculosis* genomes. Unlike the Moss primer pair (P90/P91), the Vary primer pair (150C/921) binds to all IS*900* sites in each of the type I, II, and III strains. However, there are two forward primer binding sites for both primer sets in one IS*900* locus unique to the type I strains analyzed (see Table S2). This is due to a 167-bp partial duplication of IS*900* (Fig. 4). For this study, we have designated this duplication as locus 21.5 since only the forward primer from these

TABLE 2 qPCR amplification efficiency

	Primer pair				
Strain or template	Forward	Reverse	Slope	R^2	Efficiency (%)
167	P90	P91	−3.5740047	0.9956	90.46
	P90Corr	P91	−3.6082333	0.9944	89.30
	150C	921	−3.3369762	0.9933	99.38
	JB5F	JB5R	−3.2801345	0.9954	101.77
K-10	P90	P91	−3.7656404	0.9957	84.31
	P90Corr	P91	−3.6160345	0.9938	89.04
	150C	921	−3.2797773	0.9949	101.79
	JB5F	JB5R	−3.4627333	0.9955	94.44

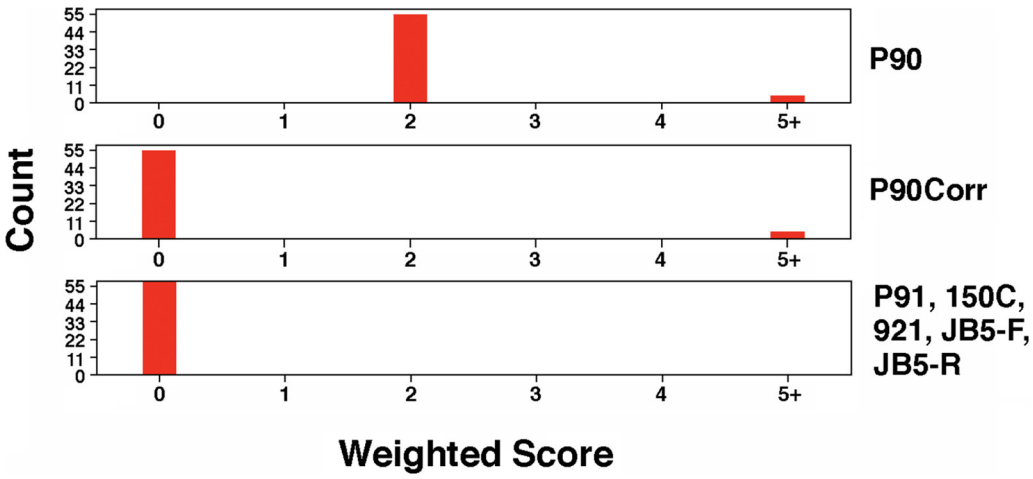

FIG 2 Graphical output from PrimerProspector showing the weighted score for each of the primers used in this study. Each primer was analyzed against 58 IS*900* loci from each of the representative subtype strains of *M. avium* subsp. *paratuberculosis* (K-10, S397, and Telford). Weighted scores give higher penalties to primers that poorly match the sequence in the 3′ region of the primer. A weighted score of 5+ indicates no primer binding while scores closest to 0 predict optimal primer performance. The top two graphs represent a single primer tested on 58 loci plotted by count versus weighted score. The bottom graph shows the identical result obtained for the remaining five primers tested. See Materials and Methods for the weighted score formula. Note that all primers used in this study except P90 and P90Corr showed a theoretically perfect weighted score of 0.

two primer pairs bind in this region (Fig. 4; see also Table S2). This extra forward primer binding site creates two amplification products for this locus only (229 and 394 bp; see Table S2). The JB5 primer pair does not bind within the 167-bp duplication, but it does flank the fluorescent probe sequence developed by Vary et al. (1) (see Fig. S1).

To determine how widespread this partial duplication is among *M. avium* subsp. *paratuberculosis* strains, available sequence reads from 439 *M. avium* subsp. *paratuberculosis* strains were aligned to the unique 400-bp query sequence derived from the Telford strain. This unique sequence is formed by the junction between the end of the partial duplication and the start of IS*900* locus 22 (see Fig. 4 and Table S3 for query sequence used to map the reads). None of the 370 type II strains contained the 167-bp duplication (see Table S3). However, the duplication is present in 62 of 63 type I strains analyzed (see Table S3). The only type I strain that did not show the partial duplication had the SRA ID SRR11839129 (see Table S3). Furthermore, this duplication was absent in 5 of 6 type III strains analyzed. The only type III

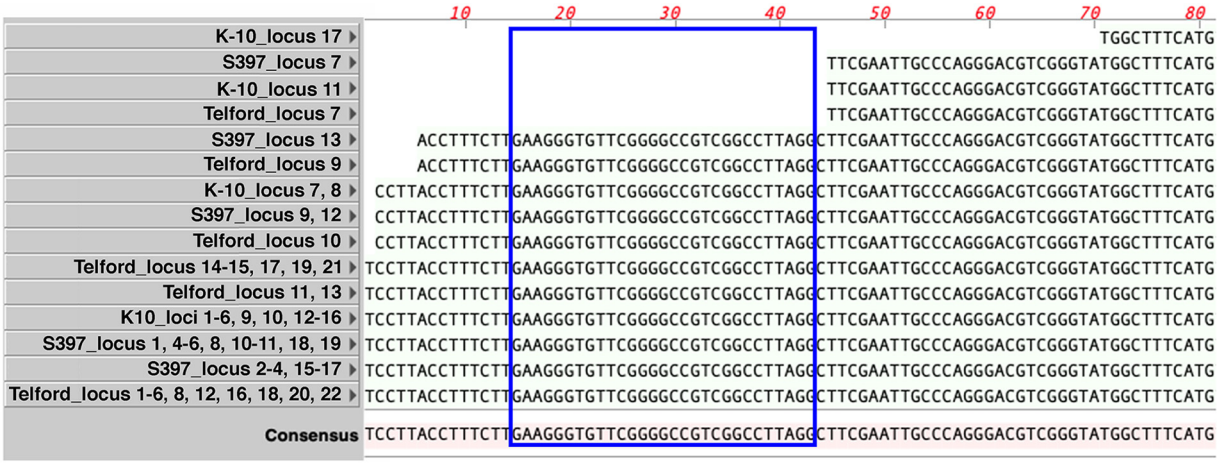

FIG 3 Sequence alignment of all 58 IS*900* loci from representative type I (Telford), II (K-10), and III (S397) strains of *M. avium* subsp. *paratuberculosis*. Shown is an alignment of the first 81 nucleotides at the 5′ end of the IS*900* element for all loci present in the representative strains. These 58 loci were binned into 15 variants and aligned using MacVector software. The consensus sequence is at the bottom and the red numbered nucleotide scale is shown across the top. The blue box shows the location of the P90Corr primer binding site. Note that deletions at four loci prevent P90 or P90Corr binding.

```
400-bp_query_S397       GGGTCCCCGATCGACAACCGTGACGGTCATGACTGTCCTTACCTTTCTTGAAGGGTGTTC 60
400-bp_query_JIII386    GGGTCCCCGATCGACAACCGTGACGGTCATGACTGTCCTTACCTTTCTTGAAGGGTGTTC 60
400-bp_query_Telford    GGGTCCCCGATCGACAACCGTGACGGTCATGACTGTCCTTACCTTTCTTGAAGGGTGTTC 60
IS900_Telford_locus11   -------------------------------------TCCTTACCTTTCTTGAAGGGTGTTC 25
167-bp_repeat_seq       -------------------------------------TCCTTACCTTTCTTGAAGGGTGTTC 25
P90-Corr                ----------------------------------------------GAAGGGTGTTC 11
150C                    ------------------------------------------------------------ 0

400-bp_query_S397       GGGGCCGTCGGCCTTAGGCTTCGAATTGCCCAGGGACGTCGGGTATGGCTTTCATGTGGT 120
400-bp_query_JIII386    GGGGCCGTCGGCCTTAGGCTTCGAATTGCCCAGGGACGTCGGGTATGGCTTTCATGTGGT 120
400-bp_query_Telford    GGGGCCGTCGGCCTTAGGCTTCGAATTGCCCAGGGACGTCGGGTATGGCTTTCATGTGGT 120
IS900_Telford_locus11   GGGGCCGTCGGCCTTAGGCTTCGAATTGCCCAGGGACGTCGGGTATGGCTTTCATGTGGT 85
167-bp_repeat_seq       GGGGCCGTCGGCCTTAGGCTTCGAATTGCCCAGGGACGTCGGGTATGGCTTTCATGTGGT 85
P90-Corr                GGGGCCGTCGGCCTTAGG---------------------------------------- 29
150C                    ------------------------------------------------------------ 0

400-bp_query_S397       TGCTGTGTTGGATGGCCGAAGGAGATTGGCCGCCCGGCGTCCCGCGACGACTCGACCGCT 180
400-bp_query_JIII386    TGCTGTGTTGGATGGCCGAAGGAGATTGGCCGCCCGGCGTCCCGCGACGACTCGACCGCT 180
400-bp_query_Telford    TGCTGTGTTGGATGGCCGAAGGAGATTGGCCGCCCGGCGTCCCGCGACGACTCGACCGCT 180
IS900_Telford_locus11   TGCTGTGTTGGATGGCCGAAGGAGATTGGCCGCCCGGCGTCCCGCGACGACTCGACCGCT 145
167-bp_repeat_seq       TGCTGTGTTGGATGGCCGAAGGAGATTGGCCGCCCGGCGTCCCGCGACGACTCGACCGCT 145
P90-Corr                ------------------------------------------------------------ 29
150C                    ----------------------------------------------------CCGCT 5

400-bp_query_S397       AATTGAGAGATGCGATTGGATCGTTGTGTAAGGACACGTCGGCGTGGTCGTCTGCTGGGT 240
400-bp_query_JIII386    AATTGAGAGATGCGATTGGATCCTTACCTTTCTTGAAGGGTGTTCGGGGCCGTCGGCCTT 240
400-bp_query_Telford    AATTGAGAGATGCGATTGGATCCTTACCTTTCTTGAAGGGTGTTCGGGGCCGTCGGCCTT 240
IS900_Telford_locus11   AATTGAGAGATGCGATTGGATCGCTGTGTAAGGACACGTCGGCGTGGTCGTCTGCTGGGT 205
167-bp_repeat_seq       AATTGAGAGATGCGATTGGATC---------------------------------------- 167
P90-Corr                ------------------------------------------------------------ 29
150C                    AATTGAGAGATGCGATTGG---------------------------------------- 24
```

FIG 4 Multiple sequence alignment of the 167-bp duplication of IS*900*. Matching 400-bp query sequences were extracted from each type I *M. avium* subsp. *paratuberculosis* genome (Telford and JIII-386) and aligned using Clustal Omega multiple sequence alignment. Note that the sequence diverges between the type I strains and S397 (a type III strain) after the duplication which demonstrates that the duplication is absent in S397. However, the sequence is identical between Telford and JIII-386. The two forward primers (P90 and 150C) are also shown to bind within the partial duplication. This duplication is shown within the red box and is flush with the 5′ start of IS*900*. It is present in all type I strains analyzed. This duplication has been designated locus 21.5 (see Table S2 in the supplemental material for coordinates). The IS*900*_Telford_locus_11 used in the alignment represents a "typical" copy of IS*900* at 1453-bp.

strain that showed the duplication was JIII-386 (Fig. 4), which has no SRA data in NCBI, but is a closed genome (32). It is unclear why the JIII-386 strain is the only type III strain to contain the duplication, but there are not enough available sequence data from type III strains ($n = 6$) to make any conclusions about the presence or absence of the duplication in that *M. avium* subsp. *paratuberculosis* subtype. In general, the duplication appears to exist primarily in type I strains and may be variably present in type III strains.

qPCR of *M. avium* subsp. *paratuberculosis* DNA. With the discovery of primer-template mismatches along with missing primer binding sequences at some IS*900* loci, it is important to test how these findings affect the IS*900* qPCR assay. DNA amplification efficiency was calculated for each primer pair on *M. avium* subsp. *paratuberculosis* genomic DNAs. The Vary and JB5 primer pairs showed the highest average amplification efficiency at 100 and 98%, respectively (Table 2). Conversely, the efficiencies using P90 and P90Corr primer pairs are 87 and 89%, respectively.

The primer pairs were also tested by qPCR on three different purified *M. avium* subsp. *paratuberculosis* genomic DNA samples standardized at 1 pg/μL, and the results showed no significant improvement when using the P90Corr primer as C_q values were virtually identical (Fig. 5). However, an improvement in average C_q that reached statistical significance was observed using JB5 and Vary primer pairs (Fig. 5). Specifically, a 2.3-C_q improvement was noted when using either the JB5 or Vary primer pairs compared to the P90 or P90Corr primer pairs (Fig. 5). This statistical difference remained between the primer pairs regardless of the DNA template. Similar results were obtained when testing nine

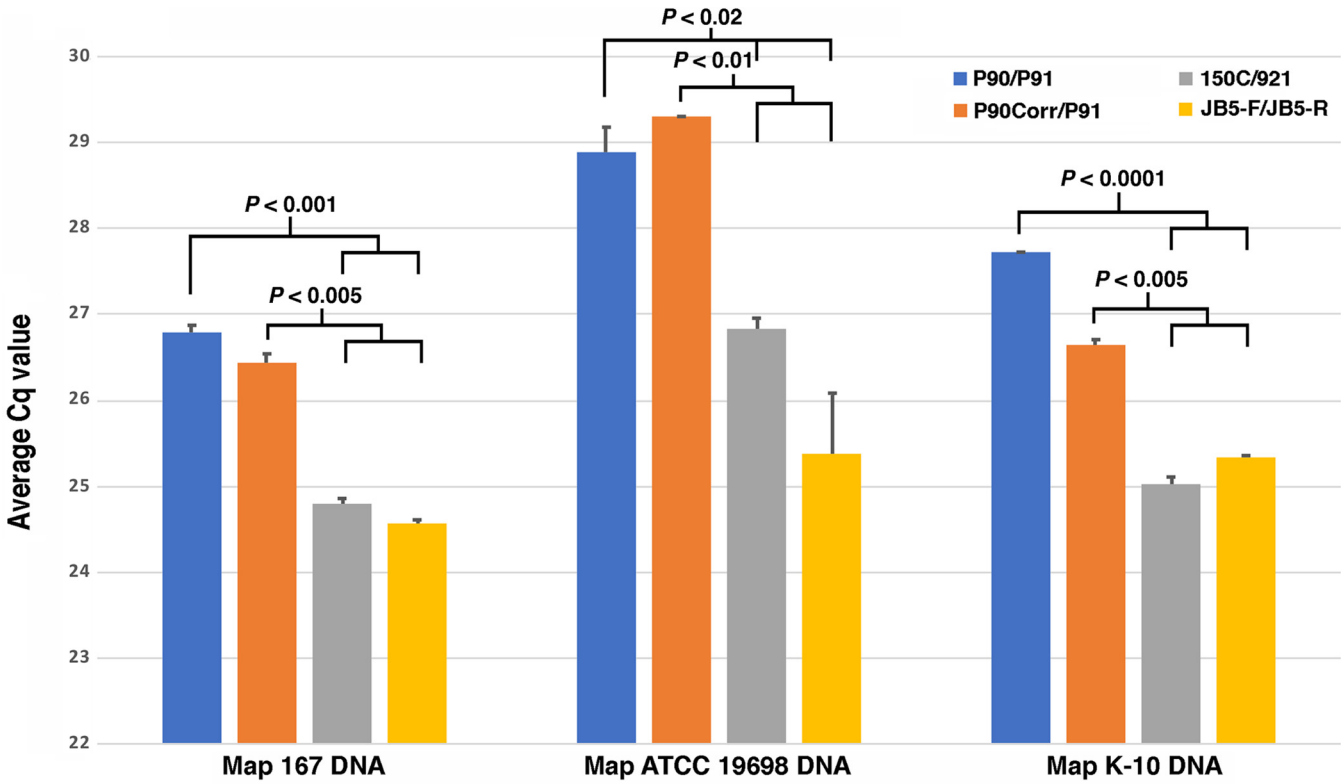

FIG 5 qPCR of purified *M. avium* subsp. *paratuberculosis* genomic DNAs. The primer pair used is indicated by the color legend at the upper right. Error bars represent the standard errors of the mean. Tukey-HSD *P* values for individual comparisons are indicated on the graph. DNA templates were standardized to 1 pg/mL by the Qubit assay.

additional *M. avium* subsp. *paratuberculosis* genomic DNAs (Table 3). The P90 and P90Corr primer sets are indistinguishable, while the Vary and JB5 primer sets detect DNA at significantly lower C_q values (Table 3). No amplification was detected using non-*M. avium* subsp. *paratuberculosis* DNA samples from the closely related *M. avium* subsp. *hominissuis* (Table 3).

qPCR of IS*900* in feces and tissues. As proof of principle, qPCR was conducted on feces and tissues from infected cows to determine amplification efficiencies on farm samples. The results show similar trends in that the Vary and JB5 primer pairs routinely outperform both the original P90/P91 and P90Corr/P91 pairs (Fig. 6). *M. avium* subsp. *paratuberculosis* DNA concentrations in these samples were calculated from the standard curve (Table 4). The

TABLE 3 qPCR results on an expanded panel of *M. avium* genomic DNAs

	Average C_q (SE)			
***M. avium* strain**	**P90/P91**	**P90Corr/P91**	**150C/921**	**JB5F/JB5R**
Subsp. *paratuberculosis*				
Ben	27.84 (0.01)	26.60 (0.18)	24.46 (0.13)	24.29 (0.06)
K-10	27.30 (0.11)	23.40 (0.66)	18.05 (0.19)	20.12 (0.15)
S397	25.36 (0.08)	23.83 (0.28)	21.98 (0.36)	21.91 (0.10)
Drew	22.63 (0.02)	20.65 (0.20)	17.74 (0.04)	18.48 (0.18)
Linda	24.00 (0.09)	24.58 (0.07)	17.65 (0.01)	17.29 (0.14)
64 1038	27.68 (0.17)	26.65 (0.12)	23.73 (0.01)	23.67 (0.15)
19698-1974	22.99 (0.11)	22.14 (0.03)	19.93 (0.06)	19.37 (0.30)
S467	24.90 (0.85)	25.19 (0.21)	19.93 (0.25)	22.07 (0.22)
6053	24.92 (0.04)	26.52 (0.10)	23.95 (0.15)	22.36 (0.20)
Avg C_q	25.29 (0.65)	24.39 (0.70)	20.82 (0.92)	21.06 (0.79)
Subsp. *hominissuis*				
3200	>40	>40	>40	>40
104	>40	>40	>40	>40

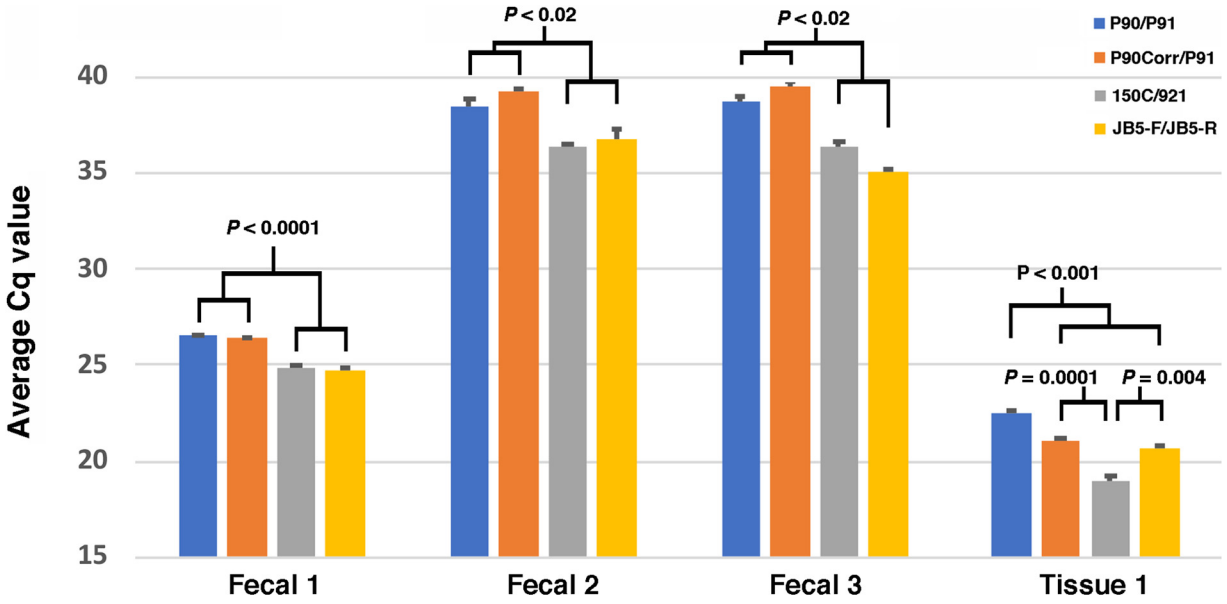

FIG 6 qPCR of fecal and tissue DNA samples of unknown concentration. The primer set used is shown by color (see legend at the top right). Error bars represent standard errors of the mean. Tukey-HSD *P* values for individual comparisons are indicated on the graph.

fecal sample pools from subclinical cows (2 and 3) are borderline positive when using the P90 or P90Corr primers with ≤1 pg *M. avium* subsp. *paratuberculosis* DNA detected in those samples. However, the Vary and JB5 primers detected >3 pg in those same samples. Pooled fecal sample 1 from clinical cows and the tissue sample from clinical cows are positive, regardless of the primers used (Table 4).

In summary, correcting a long-standing error in P90 by adding two "missing" nucleotides may marginally increase the sensitivity of IS*900* qPCR, but this increase is not significant. However, using primers that bind at all *M. avium* subsp. *paratuberculosis* loci increases the sensitivity by at least two quantification cycles.

DISCUSSION

This study highlights the practical importance of genome sequence data, as well as the robustness of DNA amplification. The original IS*900* sequence contained errors that

TABLE 4 *M. avium* subsp. *paratuberculosis* DNA concentration in fecal and tissue samples

		SQ (pg)[a]	
Sample	Primer	Avg	SD
Pooled fecal 1	P90	4,922.95	121.66
	P90Corr	5,306.08	119.14
	150C/921	15,206.69	808.22
	JB5	17,618.11	2,443.06
Pooled fecal 2	P90	1.15	0.51
	P90Corr	0.61	0.08
	150C/921	4.73	1.00
	JB5	3.72	1.72
Pooled fecal 3	P90	0.91	0.23
	P90Corr	0.46	0.10
	150C/921	4.63	1.02
	JB5	11.39	0.70
Proximal jejunum	P90	80,067.25	4,857.01
	P90Corr	237,710.96	50,996.76
	150C/921	1,005,980.26	318,155.00
	JB5	302,406.49	45,603.99

[a]Values were calculated based on the standard curve, $y = -3.2705x + 38.58$, $R^2 = 0.9947$. SQ, starting quantity in picograms.

were incorporated into the P90 primer design and was carried forward for several decades prior to whole-genome sequencing. Yet, despite these errors, a sensitive and specific PCR test was designed and used to detect *M. avium* subsp. *paratuberculosis* in that pregenomic era. Prior to the first complete genome sequence of *M. avium* subsp. *paratuberculosis* (33), the sequence of every IS*900* copy was not available. Therefore, primers were designed from a single locus of IS*900* (8) out of the 16 to 22 copies now known to be present in *M. avium* subsp. *paratuberculosis* genomes (4). Obviously, the IS*900* sequence that was originally reported by Green et al. (8) was the full-length element and not a locus with the 44- or 70-bp deletions, respectively (Fig. 3). However, the P90 primer designed from the sequence reported in that publication was missing a GC dinucleotide (see Fig. 3 [from reference 8]). Therefore, primers subsequently designed using the Green et al. sequence contained this error (23), and it was carried forward through the scientific literature (see Table S1). This error does not diminish the excellent work conducted by that research team to identify the novel IS element since it had to be cloned and sequenced by a primer walking method, and they were also successful at capturing flanking sequences for three IS*900* loci (8). At the time the work was conducted, obtaining even a kilobase of DNA sequence was manually intensive, fraught with errors, and expensive.

Although the P90 and P91 primer pair does amplify *M. avium* subsp. *paratuberculosis* DNA, these documented errors result in DNA amplification inefficiencies that can be easily avoided. There are over 80 published studies spanning three decades from 1992 through 2020 that used the P90/P91 primer pair (see Table S1). These same primers continue to be used even in recent studies, although one recent study from 2020 reports the P90 primer containing the GC dinucleotide similar to the P90Corr primer in this study (34). A few studies used the P90/P91 name designation, but the primer sequences stopped short of the GC dinucleotide, effectively avoiding the mismatch (35–38). In the present study, we examined a few commonly used IS*900* primer sets along with a newly developed PCR primer pair to determine whether we could improve the sensitivity of *M. avium* subsp. *paratuberculosis* detection. Both the Vary et al. primers and the JB5 primers demonstrated greater sensitivity of detection and higher amplification efficiencies. In conclusion, we recommend use of the Vary et al. (1) primers or the JB5F and JB5R primers for maximum *M. avium* subsp. *paratuberculosis* detection sensitivity in future studies.

This study also demonstrates that significant improvements to IS*900* detection can be obtained simply by changing primers. In this context, it is important to determine how a primer-template mismatch can affect DNA amplification results. Mismatches between the target DNA and primers are known to prevent amplification of the target (39), but in this case the 2-bp deletion in the P90 primer (Fig. 1) is clearly tolerated because it amplifies IS*900* (Fig. 5 and 6). One study demonstrated a sensitivity of detection at 50 CFU/mL in milk samples concentrated by centrifugation (40), while a second study showed detection of 1 fg/μL of purified genomic DNA (41) when using the P90/P91 pair. Thus, the historical use of P90/P91 does not invalidate any published results for *M. avium* subsp. *paratuberculosis* detection as amplification is still achieved with excellent sensitivity using these legacy primers. Adding the two missing nucleotides to create P90Corr should theoretically improve binding efficiency and sensitivity; however, any improvement was marginal since there was a nearly indistinguishable C_q value using either P90 or P90Corr forward primers.

The location of sequence mismatches within the primer can greatly affect the efficiency of amplification, which should be 100% if the number of DNA molecules doubles after each cycle (42). The detrimental effect of primer-template mismatches was previously analyzed by artificially introducing mismatches in either the primer or template of the 16S rRNA gene from *Pseudomonas aeruginosa* (39). Mismatches in the primer sequence that are located closer to the 3′ end of the primer are more detrimental to DNA amplification efficiency (30, 39). Those studies examined single base primer mismatches; however, in this study, we show the dinucleotide mismatch is located −7 and −8 nucleotides from the 3′ end of the primer (Fig. 1). Our data suggest that the mismatch was internal to the P90 primer such that detrimental effects on amplification were very small. Bru et al. (39) showed

that a single mismatch at positions −5, −6, or −8 at the 3′ end of the forward primer used to amplify the 16S rRNA gene was sufficient to lead to an underestimation of 1 log of the gene copy number. But the reverse 16S rRNA primer containing similar mismatches located more that 4 bases from the 3′ end showed no negative effect. Our data show that the dinucleotide mismatch is well tolerated in IS*900* PCR assays; however, it would be interesting to conduct additional PCR tests on more DNA samples to determine whether a statistical difference would emerge.

A significant gain in sensitivity is achieved when using primers that bind to all IS*900* loci within a given genome. When using 150C/921 or JB5F/JB5R primer pairs, C_q values were reduced by two to three cycles. These data suggest that in this case, the number of template copies available for amplification is more important than the described primer sequence errors. For *M. avium* subsp. *paratuberculosis* detection, we recommend discontinuing the use of the P90 primer along with a switch to the use of primer sets that bind within the conserved regions of IS*900*, enabling amplification from all copies in the *M.* subsp. *paratuberculosis* genome.

A 167-bp partial duplication of IS*900* was discovered when examining primer binding locations as both the P90Corr and 150C primers bind in this sequence. This duplication was absent in all 370 type II strains examined but was present in 62 of 63 type I strains analyzed. The type I strains are predominant in Australia based on *gyrAB* typing results of *M. avium* subsp. *paratuberculosis* strains from this country. Type I strains have also been identified in Saudi Arabia (10), but not in the United States. The type I CLIJ361 draft genome (43) was also examined, but since the sequence reads were unavailable, only a small fraction of the duplication could be found at the very end of contig 0234, from which nothing could be concluded. The duplication was also absent in all but one of the six type III strains analyzed. The only type III strain that contained the duplication was JIII-386. That genome has two versions in the database and the first version used a reference genome for assembly (44). If a type I strain was used for this purpose, that could have led to an assembly error. The second version used long reads and CANU assembler, suggesting a *de novo* assembly, which puts into doubt any assembly errors (44). Thus, it appears that at least one type III strain contains the 167-bp duplication. To answer the question more completely about duplication presence in type III strains, additional sequences need to be obtained for this underrepresented subtype. Our group is currently working on closing this knowledge gap by sequencing another type III strain (LN20). A search of the sequence read data from LN20 suggests the duplication is also present in that strain (unpublished results).

It was noted that primers commonly used to amplify IS*900* bind very close to the 5′ end where the deletions and duplication are located. Interestingly, the same fluorescent probe can be used for both the Vary et al. and the Moss et al. primer pairs in real-time PCR assays, which is centered around 260 bp in IS*900* (see Fig. S1). The JB5F/JB5R primers were also designed to use the same probe, thus controlling for probe variability as an effect in this study. However, it may be of interest to examine primers and probes in the central or 3′ end of IS*900* where the sequence is more stable provided *M. avium* subsp. *paratuberculosis* specificity can be retained. The specificity of both the Moss and Vary primer pairs were called into question in an early study that showed IS*900*-like sequence amplification in non-*M. avium* subsp. *paratuberculosis* mycobacteria (45), but many subsequent studies have given investigators confidence in their continued use. Nonetheless, IS*900* primers that bind near the center of the element have been developed in a few studies (5, 15, 46, 47), but these primers have not been widely adapted. One study tested centrally located IS*900* primers in a nested PCR assay that showed high specificity (15) and a second study examined fecal PCR detection in sheep, which also showed excellent specificity and sensitivity (5).

Other approaches to gain increased sensitivity of this important PCR test have shown promise, including DNA extraction methods (19), pooling or enriching samples (21, 47, 48), and testing different amplification methods (49). Likewise, targets 150 to 200 bp in length are considered best for the highest efficiency (50). The target lengths of the IS*900* amplifications in this study ranged from 229 to 415 bp (see Table S2). Since this size range is longer

TABLE 5 *M. avium* strains used in this study

Strain	*M. avium* subsp.	Subtype	Host	No. of IS*900* copies
K-10	*paratuberculosis*	II	Bovine	17
Linda	*paratuberculosis*	Unknown	Human	Unknown
Ben	*paratuberculosis*	Unknown	Human	Unknown
S397	*paratuberculosis*	III	Ovine	19
MAP4	*paratuberculosis*	II	Human	16
S467	*paratuberculosis*	III	Ovine	Unknown
Drew	*paratuberculosis*	II	Bovine	Unknown
64 1038	*paratuberculosis*	Unknown	Bovine	Unknown
19698-1974	*paratuberculosis*	II	Bovine	Unknown
6053	*paratuberculosis*	Unknown	Bovine	Unknown
104	*hominissuis*	NA[a]	Human	None
3200	*hominissuis*	NA	Swine	None
167	*paratuberculosis*	II	Bovine	Unknown

[a]NA, not applicable.

than 200 bp, it might be useful to evaluate whether primers designed to produce amplicons in the 150- to 200-bp range would further increase the efficiency of IS*900* qPCR assays.

This study provides important comparative data on the sensitivities of IS*900* primers that are currently being used in *M. avium* subsp. *paratuberculosis* research and diagnostics worldwide. Future efforts should be directed at qPCR test validation on fecal samples using robust and well-defined OIE standards, as has been done recently (27). Based on the results presented here, it is recommended to either use the Vary et al. primers or the new JB5 primer set for amplifying IS*900* in *M. avium* subsp. *paratuberculosis*.

MATERIALS AND METHODS

Genome sequences. Ref_Seq genomes of all available *M. avium* subsp. *paratuberculosis* strains were downloaded from the National Center for Biotechnology Information (NCBI) public database in February 2022. IS*900* loci were extracted from these genomes, and each was assigned a number based on their starting location within a given genome. They were numbered sequentially clockwise around each genome.

Literature search for studies using P90/P91 primers. Scopus and PubMed databases were used to conduct a literature search in September 2021 using the terms "paratuberculosis" and "IS*900* PCR." Scopus returned 413 documents and PubMed returned 321 documents. The results from each database were merged into a single list with duplicates removed. Each publication was manually inspected for the use of P90 and P91 primers. A total of 82 publications satisfied these criteria and had the primer sequences, or references to primer sequences, extracted and entered in Table S1, along with relevant bibliographic data.

Mycobacterial strains and DNA extraction. Strains used in the study were all members of the *M. avium* complex and are shown in Table 5. Mycobacterial genomic DNA extraction was conducted using a series of hydrolytic enzymes to degrade proteins and lipids prior to loading the extract onto a Qiagen 500/G genomic tip, as described previously (51). Fecal DNA extractions were performed using the bead beating method followed by DNA binding to paramagnetic beads (MagMax total nucleic acid isolation kit; Applied Biosystems, Foster City, CA), as described previously (19). Tissue samples from the mid jejunal lymph node and proximal jejunum of the same clinical cow were homogenized for DNA extractions using the gentleMACS Octo Dissociator (Miltenyi Biotech, Bergisch Gladbach, Germany), followed by centrifugation at 2,000 $\times$ *g* for 5 min to remove tissue debris. DNA was extracted using DNeasy kits (Qiagen).

Primer design and characterization. Commonly used primers for IS*900* DNA amplification were obtained from previous studies (1, 23). One primer set (JB5F/JB5R) was designed using Primer3 software, which considers thermodynamic specifications and DNA duplex stability (26, 52). All primers used in this study are shown in Table 1, and they all work with the same fluorescent probe containing a 5′ fluorophore and a 3′ quencher designed by Vary et al. (1). Primers were synthesized by Integrated DNA Technologies (IDT) using a standard desalting purification method while the probe was synthesized by IDT and purified by high-pressure liquid chromatography. To evaluate the primer-to-target mismatches, primers were tested with PrimerProspector 1.0.1 (30) using default settings. Specifically, all primer pairs were tested against a FASTA file containing all 58 IS*900* loci from Telford (type I), K-10 (type II), and S397 (type III) strains of *M. avium* subsp. *paratuberculosis*. Primer scores were calculated based on the following formula: weighted score = non-3′ mismatches $\times$ 0.40 + 3′ mismatches $\times$ 1.00 + non-3′ gaps $\times$ 1.00 + 3′ gaps $\times$ 3.00 (30). The closer the overall weighted score is to 0, the better the theoretical performance of the primer.

Bioinformatic analyses. All available *M. avium* subsp. *paratuberculosis* genomes and sequence read archive (SRA) data were downloaded from the National Center for Biotechnology Information (NCBI). The short reads were 250 bp in length from the SRA database and 300 bp for strain S397. To identify a partial duplication of IS*900*, a 400-bp Telford strain sequence spanning the duplication was used to query genome sequence reads. Reads mapping to this sequence were extracted using a k-mer approach implemented in the MIRA v4.9.6 Mirabait package (53). Using the default parameters, the extracted

reads were subsequently aligned to the reference junction sequence via the Burrows-Wheeler Aligner (BWA v0.7.17) BWA MEM algorithm. Alignment outputs were in binary alignment files (BAM files). The BAM files were sorted and indexed via SAMtools (v1.10). Read counts spanning the junction sequence were obtained by analyzing the BAM files with BEDtools (v2.30.0). Strains were considered positive for the presence of the duplication if there were more than 3 reads that spanned the junction point with a minimum of 50 aligned base pairs on both sides of the junction. Multiple sequence alignments were performed using Clustal Omega (54). Strain typing of *M. avium* subsp. *paratuberculosis* using publicly available SRA data were performed using Bash and Perl scripts to collect SNP data and compare it to established *gyrA* and *gyrB* gene references from K-10 (55) to create variant call format files. The *gyrA* and *gyrB* reference genes were used as targets for extracting reads with Mirabait as described above, and the extracted reads were aligned with BWA MEM as described. Variant calls were made using FreeBayes v1.3.6 with the default parameters.

Real-time PCR assay. Real-time PCR was performed on a 7500 Fast Sequence Detection System (Applied Biosystems) using the following reaction conditions: 1 cycle at 50°C for 2 min and 95°C for 10 min, followed by 40 cycles of denaturation at 94°C for 25 s and annealing-extension at 66°C for 1 min. The total reaction volume in each sample was 25 μL, which included 5 μL of known or unknown concentrations of template, 12.5 μL of Applied Biosystems TaqMan Environmental Master Mix 2.0, 6.88 μL of ultrapure distilled water (DNase- and RNase-free), 200 nM concentrations of each primer, and 100 nM TaqMan probe. All reactions were performed in triplicate. The 5′-fluorescein-labeled probe with a 3′-tetramethyl-rhodamine quencher was synthesized by Integrated DNA Technologies (Coralville, IA) and adapted from Vary et al. (1) (Table 1). Each individual sample was run in triplicate. A sample was considered positive if all the triplicate samples had an average quantification cycle (C_q) value below 40. All qPCR products were analyzed by electrophoresis on 1.5% agarose gels to verify the purity and expected size of the amplified products. The standard curve was run using the Vary et al. (1) primers (designated 150C and 921) on 10-fold serial dilutions of *M. avium* subsp. *paratuberculosis* K-10 purified genomic DNA ranging from 1,000 pg/μL to 0.001 pg/μL. Controls with no template DNA were included in all assays to check for contamination.

DNA amplification efficiency. For amplification efficiency calculations, standard curves were assembled for each primer pair on serial dilutions of genomic DNA extracted from two different *M. avium* subsp. *paratuberculosis* type II strains (167 and K-10). These samples were subjected to real-time PCR using the same conditions described above. DNA amplification percent efficiencies (E) were calculated using the following formula: $E = (10^{-1/\text{slope}} - 1) \times 100$ (56).

Statistical analysis. Three independent trials were conducted for all primer pairs and the average was calculated. Real-time PCR data were analyzed by one-way analysis of variance. When primer pair effects reached statistical significance ($P < 0.05$), means separation was conducted by using the Tukey-HSD test.

SUPPLEMENTAL MATERIAL

Supplemental material is available online only.

SUPPLEMENTAL FILE 1, PDF file, 0.4 MB.

SUPPLEMENTAL FILE 2, XLSX file, 0.02 MB.

SUPPLEMENTAL FILE 3, XLSX file, 0.04 MB.

SUPPLEMENTAL FILE 4, XLSX file, 0.1 MB.

ACKNOWLEDGMENT

This study was supported by the U.S. Department of Agriculture, Agricultural Research Service.

REFERENCES

1. Vary PH, Andersen PR, Green E, Hermon-Taylor J, McFadden JJ. 1990. Use of highly specific DNA probes and the polymerase chain reaction to detect *Mycobacterium paratuberculosis* in Johne's disease. J Clin Microbiol 28:933–937. https://doi.org/10.1128/jcm.28.5.933-937.1990.
2. Chater KF, Bruton CJ, Foster SG, Tobek I. 1985. Physical and genetic analysis of IS*110*, a transposable element of *Streptomyces coelicolor* A3(2). Mol Gen Genet 200:235–239. https://doi.org/10.1007/BF00425429.
3. Bannantine JP, Conde C, Bayles DO, Branger M, Biet F. 2020. Genetic diversity among *Mycobacterium avium* subspecies revealed by analysis of complete genome sequences. Front Microbiol 11:1701. https://doi.org/10.3389/fmicb.2020.01701.
4. Conde C, Price-Carter M, Cochard T, Branger M, Stevenson K, Whittington R, Bannantine JP, Biet F. 2021. Whole-genome analysis of *Mycobacterium avium* subsp. *paratuberculosis* IS*900* insertions reveals strain type-specific modalities. Front Microbiol 12:660002. https://doi.org/10.3389/fmicb.2021.660002.
5. Kawaji S, Taylor DL, Mori Y, Whittington RJ. 2007. Detection of *Mycobacterium avium* subsp. *paratuberculosis* in ovine faeces by direct quantitative PCR has similar or greater sensitivity compared to radiometric culture. Vet Microbiol 125:36–48. https://doi.org/10.1016/j.vetmic.2007.05.002.
6. Tizard ML, Moss MT, Sanderson JD, Austen BM, Hermon-Taylor J. 1992. p43, the protein product of the atypical insertion sequence IS*900*, is expressed in *Mycobacterium paratuberculosis*. J Gen Microbiol 138(Pt 8):1729–1736. https://doi.org/10.1099/00221287-138-8-1729.
7. Slana I, Alonso B, Poisson V. 2021. Chapter 3.1.16: paratuberculosis (Johne's disease), p 1–16. *In* Manual of diagnostic tests and vaccines for terrestrial animals 2022. World Organization for Animal Health, Paris, France.
8. Green EP, Tizard ML, Moss MT, Thompson J, Winterbourne DJ, McFadden JJ, Hermon-Taylor J. 1989. Sequence and characteristics of IS*900*, an insertion element identified in a human Crohn's disease isolate of *Mycobacterium paratuberculosis*. Nucleic Acids Res 17:9063–9073. https://doi.org/10.1093/nar/17.22.9063.
9. Collins DM, Gabric DM, De Lisle GW. 1989. Identification of a repetitive DNA sequence specific to *Mycobacterium paratuberculosis*. FEMS Microbiol Lett 51:175–178. https://doi.org/10.1016/0378-1097(89)90503-x.
10. Elsohaby I, Fayez M, Alkafafy M, Refaat M, Al-Marri T, Alaql FA, Al Amer AS, Abdallah A, Elmoslemany A. 2021. Serological and molecular characterization of *Mycobacterium avium* subsp. *paratuberculosis* (MAP) from sheep, goats, cattle and camels in the eastern province, Saudi Arabia. Animals (Basel)11. https://doi.org/10.3390/ani11020323.

11. Soumya MP, Pillai RM, Antony PX, Mukhopadhyay HK, Rao VN. 2009. Comparison of faecal culture and IS*900* PCR assay for the detection of *Mycobacterium avium* subsp. *paratuberculosis* in bovine faecal samples. Vet Res Commun 33:781–791. https://doi.org/10.1007/s11259-009-9226-3.
12. Millar D, Ford J, Sanderson J, Withey S, Tizard M, Doran T, Hermon-Taylor J. 1996. IS*900* PCR to detect *Mycobacterium paratuberculosis* in retail supplies of whole pasteurized cows' milk in England and Wales. Appl Environ Microbiol 62:3446–3452. https://doi.org/10.1128/aem.62.9.3446-3452.1996.
13. Jayarao BM, Pillai SR, Wolfgang DR, Griswold DR, Rossiter CA, Tewari D, Burns CM, Hutchinson LJ. 2004. Evaluation of IS*900*-PCR assay for detection of *Mycobacterium avium* subspecies *paratuberculosis* infection in cattle using quarter milk and bulk tank milk samples. Foodborne Pathog Dis 1:17–26. https://doi.org/10.1089/153531404772914428.
14. Slana I, Liapi M, Moravkova M, Kralova A, Pavlik I. 2009. *Mycobacterium avium* subsp. *paratuberculosis* in cow bulk tank milk in Cyprus detected by culture and quantitative IS*900* and F57 real-time PCR. Prev Vet Med 89:223–226. https://doi.org/10.1016/j.prevetmed.2009.02.020.
15. Bull TJ, McMinn EJ, Sidi-Boumedine K, Skull A, Durkin D, Neild P, Rhodes G, Pickup R, Hermon-Taylor J. 2003. Detection and verification of *Mycobacterium avium* subsp. *paratuberculosis* in fresh ileocolonic mucosal biopsy specimens from individuals with and without Crohn's disease. J Clin Microbiol 41:2915–2923. https://doi.org/10.1128/JCM.41.7.2915-2923.2003.
16. Mobius P, Luyven G, Hotzel H, Kohler H. 2008. High genetic diversity among *Mycobacterium avium* subsp. *paratuberculosis* strains from German cattle herds shown by combination of IS*900* restriction fragment length polymorphism analysis and mycobacterial interspersed repetitive unit-variable-number tandem-repeat typing. J Clin Microbiol 46:972–981. https://doi.org/10.1128/JCM.01801-07.
17. Barkema HW, Orsel K, Nielsen SS, Koets AP, Rutten V, Bannantine JP, Keefe GP, Kelton DF, Wells SJ, Whittington RJ, Mackintosh CG, Manning EJ, Weber MF, Heuer C, Forde TL, Ritter C, Roche S, Corbett CS, Wolf R, Griebel PJ, Kastelic JP, De Buck J. 2018. Knowledge gaps that hamper prevention and control of *Mycobacterium avium* subspecies *paratuberculosis* infection. Transbound Emerg Dis 65(Suppl 1):125–148. https://doi.org/10.1111/tbed.12723.
18. Whittington RJ, Marsh IB, Taylor PJ, Marshall DJ, Taragel C, Reddacliff LA. 2003. Isolation of *Mycobacterium avium* subsp *paratuberculosis* from environmental samples collected from farms before and after destocking sheep with paratuberculosis. Aust Vet J 81:559–563. https://doi.org/10.1111/j.1751-0813.2003.tb12887.x.
19. Leite FL, Stokes KD, Robbe-Austerman S, Stabel JR. 2013. Comparison of fecal DNA extraction kits for the detection of *Mycobacterium avium* subsp. *paratuberculosis* by polymerase chain reaction. J Vet Diagn Invest 25:27–34. https://doi.org/10.1177/1040638712466395.
20. Fock-Chow-Tho D, Topp E, Ibeagha-Awemu EA, Bissonnette N. 2017. Comparison of commercial DNA extraction kits and quantitative PCR systems for better sensitivity in detecting the causative agent of paratuberculosis in dairy cow fecal samples. J Dairy Sci 100:572–581. https://doi.org/10.3168/jds.2016-11384.
21. Fawzy A, Eisenberg T, El-Sayed A, Zschock M. 2015. Improvement of sensitivity for *Mycobacterium avium* subsp. *paratuberculosis* (MAP) detection in bovine fecal samples by specific duplex F57/IC real-time and conventional IS*900* PCRs after solid culture enrichment. Trop Anim Health Prod 47:721–726. https://doi.org/10.1007/s11250-015-0784-9.
22. Sevilla IA, Garrido JM, Molina E, Geijo MV, Elguezabal N, Vazquez P, Juste RA. 2014. Development and evaluation of a novel multicopy-element-targeting triplex PCR for detection of *Mycobacterium avium* subsp. *paratuberculosis* in feces. Appl Environ Microbiol 80:3757–3768. https://doi.org/10.1128/AEM.01026-14.
23. Moss MT, Sanderson JD, Tizard ML, Hermon-Taylor J, el-Zaatari FA, Markesich DC, Graham DY. 1992. Polymerase chain reaction detection of *Mycobacterium paratuberculosis* and *Mycobacterium avium* subsp *silvaticum* in long term cultures from Crohn's disease and control tissues. Gut 33:1209–1213. https://doi.org/10.1136/gut.33.9.1209.
24. Ye J, Coulouris G, Zaretskaya I, Cutcutache I, Rozen S, Madden TL. 2012. Primer-BLAST: a tool to design target-specific primers for polymerase chain reaction. BMC Bioinformatics 13:134. https://doi.org/10.1186/1471-2105-13-134.
25. Thornton B, Basu C. 2015. Rapid and simple method of qPCR primer design. Methods Mol Biol 1275:173–179. https://doi.org/10.1007/978-1-4939-2365-6_13.
26. Untergasser A, Cutcutache I, Koressaar T, Ye J, Faircloth BC, Remm M, Rozen SG. 2012. Primer3–new capabilities and interfaces. Nucleic Acids Res 40:e115. https://doi.org/10.1093/nar/gks596.
27. Russo S, Giorgio G, Leo S, Arrigoni N, Garbarino C, Ricchi M. 2022. Validation of IS*900*- qPCR assay to assess the presence of *Mycobacterium avium* subs. *paratuberculosis* in faecal samples according to the OIE procedure. Prev Vet Med 208:105732. https://doi.org/10.1016/j.prevetmed.2022.105732.
28. Mobius P, Hotzel H, Rassbach A, Kohler H. 2008. Comparison of 13 single-round and nested PCR assays targeting IS*900*, ISMav2, f57 and locus 255 for detection of *Mycobacterium avium* subsp. *paratuberculosis*. Vet Microbiol 126:324–333. https://doi.org/10.1016/j.vetmic.2007.07.016.
29. Semret M, Turenne CY, Behr MA. 2006. Insertion sequence IS*900* revisited. J Clin Microbiol 44:1081–1083. https://doi.org/10.1128/JCM.44.3.1081-1083.2006.
30. Walters WA, Caporaso JG, Lauber CL, Berg-Lyons D, Fierer N, Knight R. 2011. PrimerProspector: de novo design and taxonomic analysis of barcoded polymerase chain reaction primers. Bioinformatics 27:1159–1161. https://doi.org/10.1093/bioinformatics/btr087.
31. Castellanos E, Aranaz A, de Juan L, Alvarez J, Rodriguez S, Romero B, Bezos J, Stevenson K, Mateos A, Dominguez L. 2009. Single nucleotide polymorphisms in the IS*900* sequence of *Mycobacterium avium* subsp. *paratuberculosis* are strain type specific. J Clin Microbiol 47:2260–2264. https://doi.org/10.1128/JCM.00544-09.
32. Wibberg D, Price-Carter M, Ruckert C, Blom J, Mobius P. 2020. Complete genome sequence of ovine *Mycobacterium avium* subsp. *paratuberculosis* strain JIII-386 (MAP-S/type III) and Its comparison to MAP-S/type I, MAP-C, and M. avium complex genomes. Microorganisms 9. https://doi.org/10.3390/microorganisms9010070.
33. Li L, Bannantine JP, Zhang Q, Amonsin A, May BJ, Alt D, Banerji N, Kanjilal S, Kapur V. 2005. The complete genome sequence of *Mycobacterium avium* subspecies *paratuberculosis*. Proc Natl Acad Sci U S A 102:12344–12349. https://doi.org/10.1073/pnas.0505662102.
34. Foddai ACG, Grant IR. 2020. A novel one-day phage-based test for rapid detection and enumeration of viable *Mycobacterium avium* subsp. *paratuberculosis* in cows' milk. Appl Microbiol Biotechnol 104:9399–9412. https://doi.org/10.1007/s00253-020-10909-0.
35. O'Shea B, Khare S, Bliss K, Klein P, Ficht TA, Adams LG, Rice-Ficht AC. 2004. Amplified fragment length polymorphism reveals genomic variability among *Mycobacterium avium* subsp. *paratuberculosis* isolates. J Clin Microbiol 42:3600–3606. https://doi.org/10.1128/JCM.42.8.3600-3606.2004.
36. Khare S, Ficht TA, Santos RL, Romano J, Ficht AR, Zhang S, Grant IR, Libal M, Hunter D, Adams LG. 2004. Rapid and sensitive detection of *Mycobacterium avium* subsp. *paratuberculosis* in bovine milk and feces by a combination of immunomagnetic bead separation-conventional PCR and real-time PCR. J Clin Microbiol 42:1075–1081. https://doi.org/10.1128/JCM.42.3.1075-1081.2004.
37. Herthnek D, Englund S, Willemsen PT, Bolske G. 2006. Sensitive detection of *Mycobacterium avium* subsp. *paratuberculosis* in bovine semen by real-time PCR. J Appl Microbiol 100:1095–1102. https://doi.org/10.1111/j.1365-2672.2006.02924.x.
38. Paolicchi F, Cirone K, Morsella C, Gioffre A. 2012. First isolation of *Mycobacterium avium* subsp *paratuberculosis* from commercial pasteurized milk in Argentina. Braz J Microbiol 43:1034–1037. https://doi.org/10.1590/s1517-83822012000300028.
39. Bru D, Martin-Laurent F, Philippot L. 2008. Quantification of the detrimental effect of a single primer-template mismatch by real-time PCR using the 16S rRNA gene as an example. Appl Environ Microbiol 74:1660–1663. https://doi.org/10.1128/AEM.02403-07.
40. Grant IR, Pope CM, O'Riordan LM, Ball HJ, Rowe MT. 2000. Improved detection of *Mycobacterium avium* subsp. *paratuberculosis* in milk by immunomagnetic PCR. Vet Microbiol 77:369–378. https://doi.org/10.1016/s0378-1135(00)00322-9.
41. Marsh IB, Whittington RJ. 2001. Progress towards a rapid polymerase chain reaction diagnostic test for the identification of *Mycobacterium avium* subsp. *paratuberculosis* in faeces. Mol Cell Probes 15:105–118. https://doi.org/10.1006/mcpr.2001.0345.
42. Kralik P, Ricchi M. 2017. A basic guide to real-time PCR in microbial diagnostics: definitions, parameters, and everything. Front Microbiol 8:108. https://doi.org/10.3389/fmicb.2017.00108.
43. Wynne JW, Bull TJ, Seemann T, Bulach DM, Wagner J, Kirkwood CD, Michalski WP. 2011. Exploring the zoonotic potential of *Mycobacterium avium* subspecies *paratuberculosis* through comparative genomics. PLoS One 6:e22171. https://doi.org/10.1371/journal.pone.0022171.
44. Mobius P, Holzer M, Felder M, Nordsiek G, Groth M, Kohler H, Reichwald K, Platzer M, Marz M. 2015. Comprehensive insights in the *Mycobacterium avium* subsp. *paratuberculosis* genome using new WGS data of sheep strain JIII-386 from Germany. Genome Biol Evol https://doi.org/10.1093/gbe/evv154.
45. Englund S, Bolske G, Johansson KE. 2002. An IS*900*-like sequence found in a Mycobacterium sp. other than *Mycobacterium avium* subsp. *paratuberculosis*. FEMS Microbiol Lett 209:267–271. https://doi.org/10.1111/j.1574-6968.2002.tb11142.x.

46. Donaghy JA, Johnston J, Rowe MT. 2011. Detection of *Mycobacterium avium* ssp. *paratuberculosis* in cheese, milk powder and milk using IS*900* and f57-based qPCR assays. J Appl Microbiol 110:479–489. https://doi.org/10.1111/j.1365-2672.2010.04905.x.
47. Ly A, Dhand NK, Sergeant ESG, Marsh I, Plain KM. 2019. Determining an optimal pool size for testing beef herds for Johne's disease in Australia. PLoS One 14:e0225524. https://doi.org/10.1371/journal.pone.0225524.
48. Mita A, Mori Y, Nakagawa T, Tasaki T, Utiyama K, Mori H. 2016. Comparison of fecal pooling methods and DNA extraction kits for the detection of *Mycobacterium avium* subspecies *paratuberculosis*. Microbiologyopen 5:134–142. https://doi.org/10.1002/mbo3.318.
49. Sonawane GG, Tripathi BN. 2013. Comparison of a quantitative real-time polymerase chain reaction (qPCR) with conventional PCR, bacterial culture and ELISA for detection of subsp. infection in sheep showing pathology of Johne's disease. Springerplus 2:45. https://doi.org/10.1186/2193-1801-2-45.
50. Van Holm W, Ghesquiere J, Boon N, Verspecht T, Bernaerts K, Zayed N, Chatzigiannidou I, Teughels W. 2021. A viability quantitative PCR dilemma: are longer amplicons better? Appl Environ Microbiol 87:e0265320. https://doi.org/10.1128/AEM.02653-20.
51. Bannantine JP, Baechler E, Zhang Q, Li L, Kapur V. 2002. Genome scale comparison of *Mycobacterium avium* subsp. *paratuberculosis* with *Mycobacterium avium* subsp. *avium* reveals potential diagnostic sequences. J Clin Microbiol 40:1303–1310. https://doi.org/10.1128/JCM.40.4.1303-1310.2002.
52. Koressaar T, Remm M. 2007. Enhancements and modifications of primer design program Primer3. Bioinformatics 23:1289–1291. https://doi.org/10.1093/bioinformatics/btm091.
53. Cock PJ, Gruning BA, Paszkiewicz K, Pritchard L. 2013. Galaxy tools and workflows for sequence analysis with applications in molecular plant pathology. PeerJ 1:e167. https://doi.org/10.7717/peerj.167.
54. Sievers F, Wilm A, Dineen D, Gibson TJ, Karplus K, Li W, Lopez R, McWilliam H, Remmert M, Soding J, Thompson JD, Higgins DG. 2011. Fast, scalable generation of high-quality protein multiple sequence alignments using Clustal Omega. Mol Syst Biol 7:539. https://doi.org/10.1038/msb.2011.75.
55. Castellanos E, Aranaz A, Romero B, de Juan L, Alvarez J, Bezos J, Rodriguez S, Stevenson K, Mateos A, Dominguez L. 2007. Polymorphisms in *gyrA* and *gyrB* genes among *Mycobacterium avium* subsp. *paratuberculosis* type I, II, and III isolates. J Clin Microbiol 45:3439–3442. https://doi.org/10.1128/JCM.01411-07.
56. Sreedharan SP, Kumar A, Giridhar P. 2018. Primer design and amplification efficiencies are crucial for reliability of quantitative PCR studies of caffeine biosynthetic *N*-methyltransferases in coffee. 3 Biotech 8:467. https://doi.org/10.1007/s13205-018-1487-5.